Available online at www.sciencedirect.com
SCIENCE DIRECT®

Journal of the European Ceramic Society 23 (2003) 1935–1941
www.elsevier.com/locate/jeurceramsoc

Lead germanium oxide sinter-assisted PZT composite thick films

F.F.C. Duval, R.A. Dorey, Q. Zhang, R.W. Whatmore

School of Industrial and Manufacturing Science, Cranfield University, Bedfordshire MK43 0AL, UK

Received 20 March 2002; received in revised form 15 October 2002; accepted 20 October 2002

Abstract

Thick films of niobium doped lead zirconate titanate (PNZT) were prepared from a sol-gel/PZT powder composite slurry. The effects of adding different amounts of sol-gel derived lead germanium oxide (PGO) as sintering aid were examined. Four layers of composite, with intermediate sol infiltrations, were deposited by spinning onto $Pt/Ti/SiO_2/Si$ substrates followed by drying and annealing. Addition of PGO enhanced the densification process at a temperature as low as 770 °C. It resulted in an increase in the film properties that depended upon the level of PGO addition. Film properties were assessed by measuring the capacitance and dielectric loss. $d_{33,f}$ and $e_{31,f}$ piezoelectric coefficient measurements were carried out after poling at 10 V/μm for 5 min at 130 °C. A maximum relative permittivity of 500 was observed between 5 and 8 wt.% PGO addition. The maximum in $d_{33,f}$ was found to be about 40 pC/N. Additions between 7 and 10 wt.% PGO led to the maximum $e_{31,f}$ piezoelectric coefficient of about -1.5 C/m^2.

Keywords: Composites; Dielectric properties; $Pb_5Ge_3O_{11}$; Piezoelectric properties; PZT; Sintering aid; Sol-gel processes

1. Introduction

Lead zirconate titanate (PZT) thick film manufacture has been widely investigated over the last 10 years.[1–3] Many applications, such as high frequency ultrasonic transducers require film thicknesses greater than several tens of microns.[4] Screen-printing is widely used to deposit films 10–50 μm thick but is not very suitable for printing onto silicon substrates due to the high sintering temperatures required. Films between 9 and 60 μm thick can be produced by spin-coating at low temperatures through the use of a composite slurry.[5] Barrow et al. [6] were the first to describe the benefits of using an undoped sol-gel/commercial PZT powder slurry to deposit a crack-free composite layer several microns thick. Corker et al. [7] described the use of the composite process in association with a PbO/Cu_2O sintering aid to achieve high density doped PZT films, in this case matching the composition of the sol to that of the powder. Along with the use of sintering aids, sol infiltration has been employed successfully to produce 'hard' doped PZT thick films with high densities.[8]

The viscosity of the composite slurry is an important factor to control. Ideally the viscosity should be as high as possible to deposit thick layers, but should not result in cracking. Corker et al. [7] showed that the viscosity of the composite can be controlled by adjusting the pH: ceramic powder particles can be stabilised by imparting a positive or negative charge depending on the pH of the medium. Therefore, acetic acid was incorporated into the composite slurry to control the viscosity and the wetting behaviour during deposition. However, it was found that the PbO/Cu_2O sintering aid was not compatible with an acidified composite slurry: a Cu^{2+}/Cu^{+} reduction process occurs in the acidic medium, leading to the formation of CuO that does not form a liquid phase with PbO at a suitable low temperature. Lead germanium oxide is a good candidate for a low temperature sintering aid because it has a melting point of 740 °C. $Pb_5Ge_3O_{11}$ is also ferroelectric with a moderate relative permittivity at room temperature (35–40),[9] which may help to maintain the dielectric properties of the resulting multiphase film.

This paper examines the manufacture of 'soft' doped PZT sol/PZT powder composite thick films using sintering aid and sol infiltration. Different additions of

E-mail address: f.f.c.duval@cranfield.ac.uk (F.F.C. Duval).

0955-2219/03/$ - see front matter
PII: S0955-2219(02)00417-X

PGO, ranging from 2 to 12 wt.%, were examined. Electric and piezoelectric properties of the films will be discussed along with the microstructural features.

2. Experimental procedures

2.1. Sol-gel synthesis

The niobium doped $Pb(Zr_{0.52}Ti_{0.48})O_3$ sol used in this work was produced from high purity reagents. The complete synthesis is described in Fig. 1. Lead acetate trihydrate (Fisher, 99.5%), zirconium *n*-propoxide (Aldrich, 75 wt.% solution in 1-propanol), titanium isopropoxide (Aldrich, 99.99%) and niobium ethoxide (Inorgtech, 99.99%) were used as precursors. The solvent chosen was ethanol as an alternative to the toxic 2-methoxyethanol used in previous work.[8] A 2 mol% niobium-doped PZT sol with a 10 mol% lead excess was produced. The sol exhibited a pH of approximately 7, a density of 0.9 g/cm^3, a viscosity of 0.02 poise and a concentration of 0.4 M.

2.2. Lead germanium oxide powder synthesis

The lead germanium oxide, with a composition of $Pb_5Ge_3O_{11}$, was also synthesised through a sol-gel process. First a sol was produced from lead acetate trihydrate and germanium isopropoxide (Chemat Technology, 99.99%) as described in Fig. 2. The sol was then hydrolysed by adding 2 ml of distilled water and heating at 85 °C for 3 h to promote the formation of a gel. Finally the gel was calcined at 600 °C for 2 h.

The PGO powder was analysed by X-ray diffraction using a Siemens D-5005 diffractometer and compared with the standard pattern.[10] Fig. 3 indicates that crystallised hexagonal PGO was obtained. The extra peaks originated from the tape used to mount the PGO powder during XRD analysis.

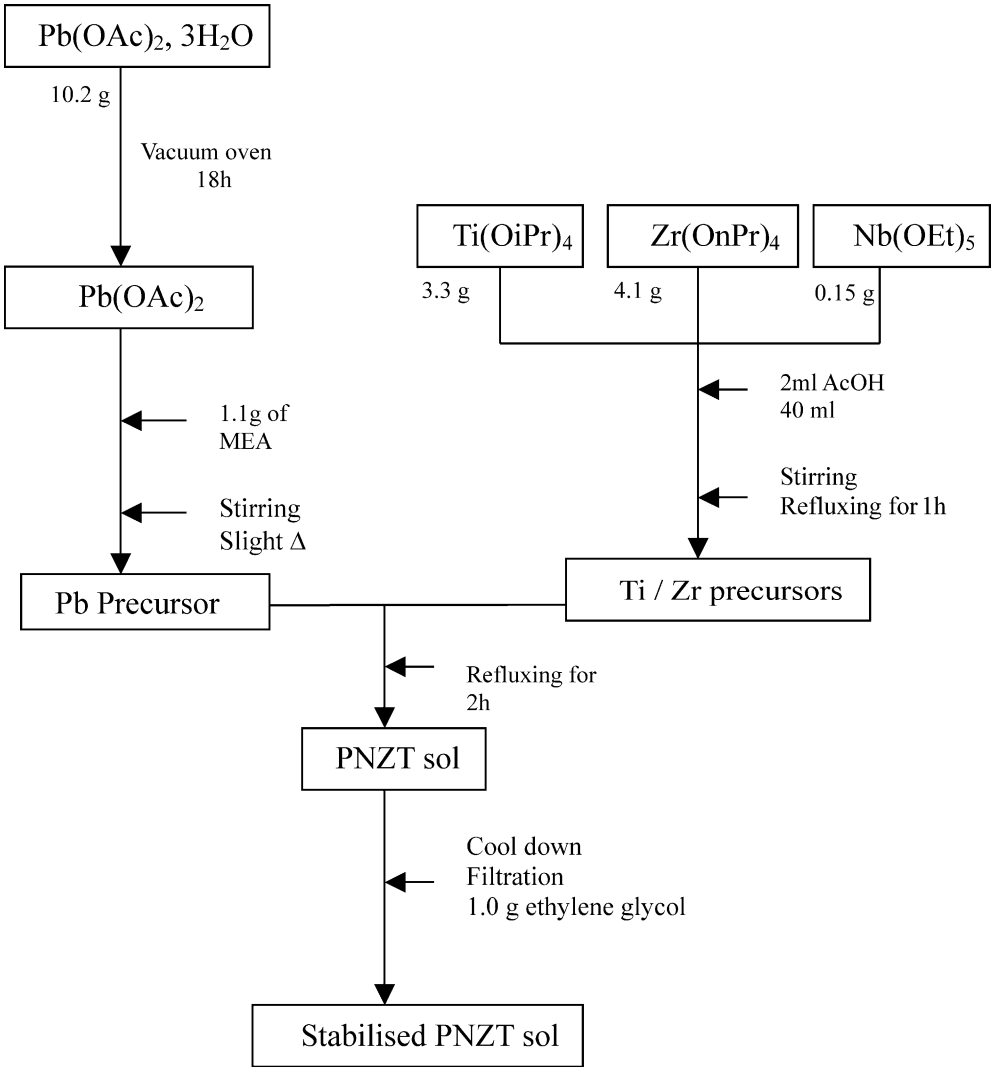

Fig. 1. Flowchart of the niobium-doped PZT sol-gel production process.

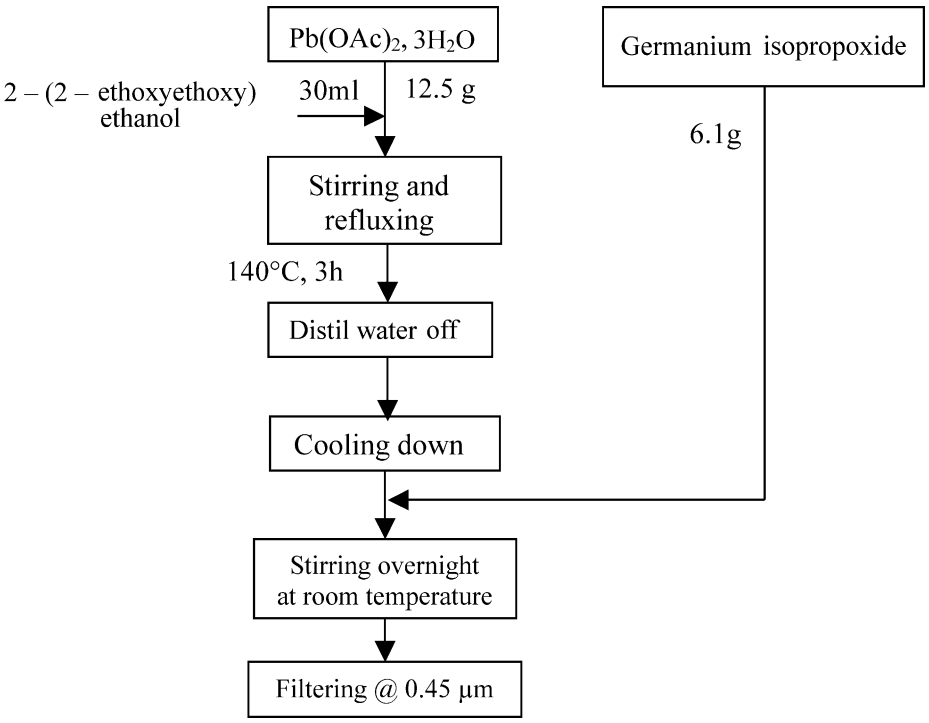

Fig. 2. Flowchart of the PGO sol-gel production process.

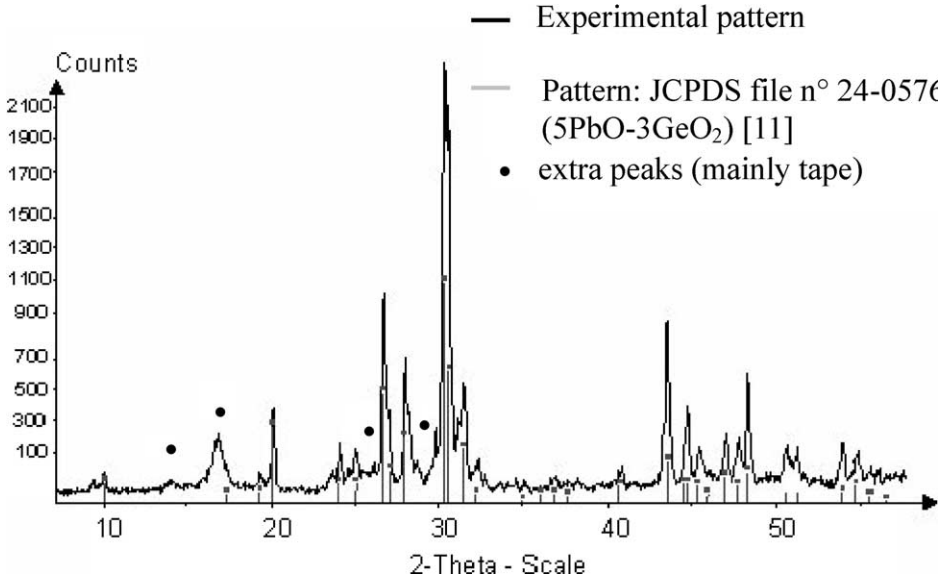

Fig. 3. X-ray pattern of the PGO powder and the standard pattern.

2.3. Composite slurry production and films deposition

The composite slurries were produced by mixing the PZT sol and a 'soft' doped PZT powder (PZ 27, Ferroperm, DK). Several additives were then added: a dispersant KR55 (Ken-React Lica 38, KenRich) (2 wt.% relative to the PZT powder mass) to ensure homogeneous dispersion of the PZT powder; the PGO sintering aid in different proportions, 2, 3, 5, 7, 8, 10 and 12 wt.% relative to the PZT powder mass; and acetic acid, representing 33.3 v/v% of the liquid phase (sol and acetic acid). The process was completed by ball-milling the suspension for 24 h. A composite slurry was produced, such that for each millilitre of liquid phase (sol + acetic acid) 1.5 g of PZT powder was added (i.e. 1.5 g/ml). Composite deposition was performed on platinised silicon wafers ($Pt/Ti/SiO_2/Si$). Prior to use, the substrates were cleaned with acetone and then with isopropanol, ensuring that a constant flow of solvent was maintained. Finally, the samples were cleaned using an

oxygen plasma (PT 7160 RF Plasma Barrel Etcher) for 3 min at 1.5×10^{-2} mbar. The substrates were fully coated with the suspension and then spun at 2000 rpm for 30 s. The as-deposited film was then dried at 200 °C for 60 s and pyrolysed at 450 °C for 15 s to remove all of the organic components. The porous composite layer was then infiltrated 4 times with sol. Each infiltration step was followed by a drying and pyrolysis step before the next infiltration step. The next composite layer was then deposited and the process was repeated until the desired thickness was obtained. The process was completed with a Rapid Thermal Annealing (RTA) treatment to fully develop the perovskite phase.

The nomenclature to describe the experimental conditions is such that:

4[C + 4S]770C30M,

relates to a four-layer composite film infiltrated with four layers of sol per layer of composite and annealed at 770° Celsius for 30 min; C and S relate to the composite and sol respectively.

2.4. Microstructure evaluation

A scanning electron microscope (ABT-55) was used to examine the surface finish of the films and the polished cross sections. The surface finish was assessed by measuring the mean roughness (Ra) using a Dektak® Surface Profiler. The area crack density, along with the film porosity, were measured using Leica Q500 MC Image analysis software. The area crack density was defined as the ratio between the area represented by the cracks and the total area. The porosity was evaluated for each layer of composite by evaluating the area of holes relative to the total area.

2.5. Electrical and piezoelectric coefficients measurements

Gold chromium electrodes were deposited onto the surface of the films by vacuum evaporation using an Edward Evaporator E480. The capacitance and dielectric loss were measured before poling using a Wayne Kerr 6425 Analyser employing a low voltage of 0.1 V and a frequency of 1 kHz. Film thicknesses were evaluated in cross section using an optical microscope. The samples were poled at 130 °C for 5 min. The voltage was increased stepwise to determine the $d_{33,f}$ saturation values, as shown in Fig. 4, using a Berlincourt type piezometer (Takecontrol PM 25). The $e_{31,f}$ (the subscript f refers to the effective film value) piezoelectric coefficients were also determined using the piezometer following the method described by Southin et al. [11] The technique consists of supporting the sample on a ring and applying a point load in the centre such that a '31' contribution is generated. Therefore, the actual d' value measured by the piezometer is the sum of both transverse and longitudinal effects such that $d' = d_{33} + e_{31,f} * f(\sigma_r,\sigma_h)$. The $e_{31,f}$ piezoelectric coefficient was calculated from this equation as well as the bulk d_{33} coefficient. This is the coefficient that would be obtained from the film if it was not clamped to the substrate. This is referred to in the text, as the extrapolated d_{33} value for the film.

3. Results and discussion

The microstructural features of the films were evaluated by examining surface finish and polished cross-sections. The films were porous, exhibiting vertical cracks (Fig. 5) that were not continuous across the total thickness of the film. SEM photomicrographs also showed that the sol did not completely infiltrate the layers of composite. This resulted in the formation of thin discrete layers of sol. The level of porosity gradually increased from the bottom to the top layer as shown in Fig. 6. It can be seen that the level of porosity was not reduced when adding more than 5 wt.% PGO. It was found that the crack area density did not depend on the level of PGO addition: 10% was the average area crack density (Fig. 7). This is reasonable as crack formation is thought to occur during the spinning and drying stage when the sintering aid is not active. The mean roughness was found to be about 0.5 μm, which is equal to the average grain size, indicating that surface roughness is limited by the size of the PZT particles employed in the composite.

The relative permittivity, as a function of the level of PGO, is shown in Fig. 8. The observed values were lower than those reported for bulk PZ 27 (1800).[12] This can be mainly ascribed to the level of porosity. When adding PGO up to 5 wt.%, a slight increase in the relative permittivity was observed as a denser structure was achieved due to the enhanced densification kinetics and the replacement of the air medium by the PGO liquid phase ($\varepsilon_{PGO} = 36$–41[9]). Adding more PGO enhanced the sintering process further but would also result in the presence of more low dielectric material which would

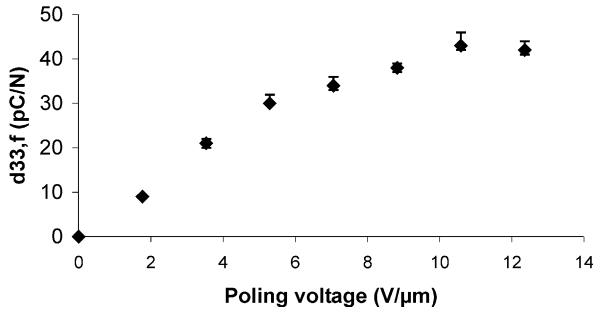

Fig. 4. $d_{33,f}$ Values as function of the poling voltage for a 4[C + 4S] 5 wt.% PGO film.

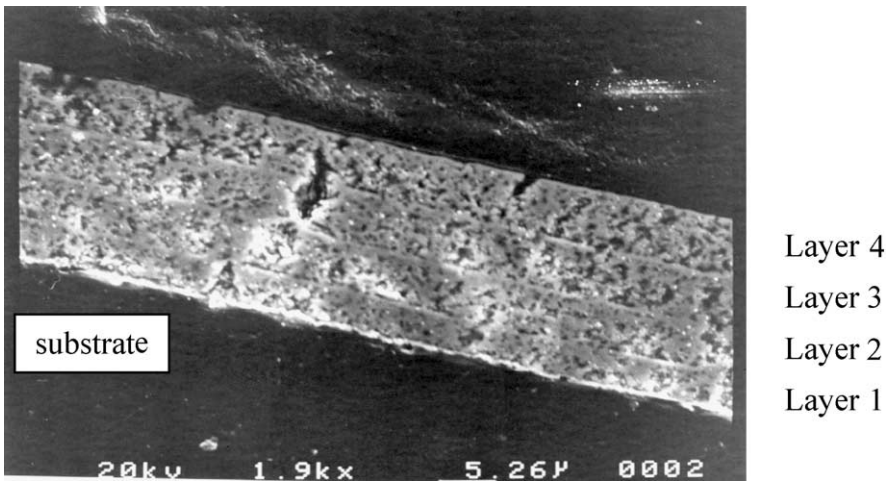

Fig. 5. Polished cross section SEM photomicrograph of a 4[C+4S], PGO 5 wt.%.

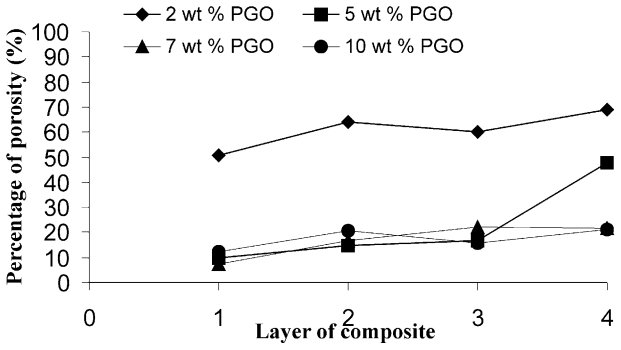

Fig. 6. Effect of PGO on the film porosity.

have a detrimental effect on the value of relative permittivity observed. Hayashi et al. [13] reported the presence of a PGO/PZT liquid secondary phase at sintering temperatures less than 950 °C for PGO-added PZT ceramics which leads to the deterioration of the ferroelectric properties.

When examining the variations in the piezoelectric coefficients (Figs. 9–11) it was found that the $d_{33,f}$ coefficient did not change significantly with PGO addition. A slight increase in $d_{33,f}$ was observed up to 5 wt.% PGO. With more than 5wt.% PGO, a small reduction occurred as more low piezoelectric coefficient material was incorporated. The values ranged from 30 to 45 pC/N with the maximum for a 5 wt.% PGO addition. The piezoelectric coefficient $e_{31,f}$ showed a 40% increase from 0 up to 7 wt.% PGO addition to reach a plateau that then decreased as PZT grains may be coated with PGO liquid phase. The 'extrapolated' d_{33} values followed the same trend as the $e_{31,f}$ to reach values between 60 and 80 pC/N. It was observed that the increase in $e_{31,f}$ followed the increase in film density with increasing PGO addition, while $d_{33,f}$ did not. The structure of the films is essentially the same as a 3-3 or 3-0 composite with the second phase, air, being either 'connected' in the high-porosity 3-3 case, or 'unconnected' at higher

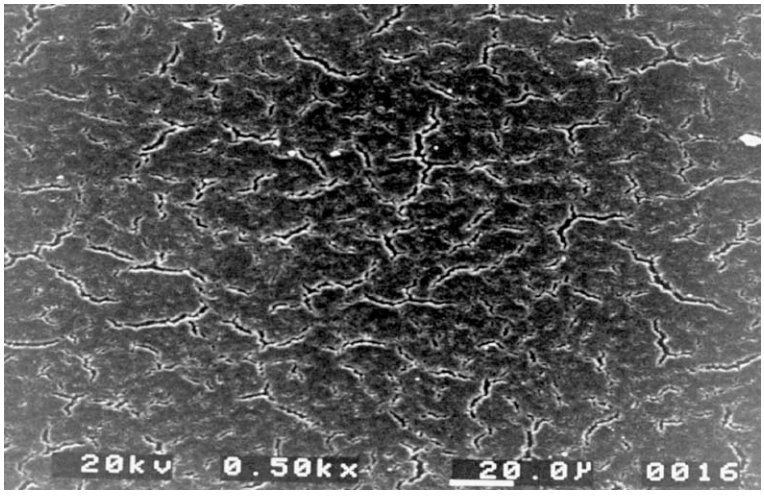

Fig. 7. Surface SEM microphotograph of 4[C+4S], PGO 5 wt.%.

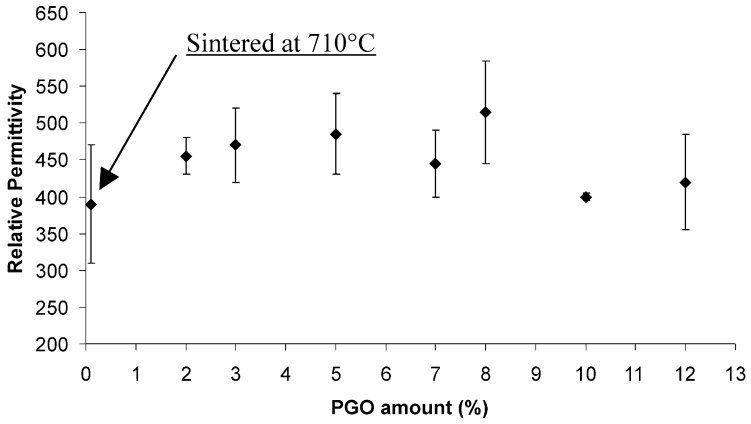

Fig. 8. Effect of PGO on the relative permittivity.

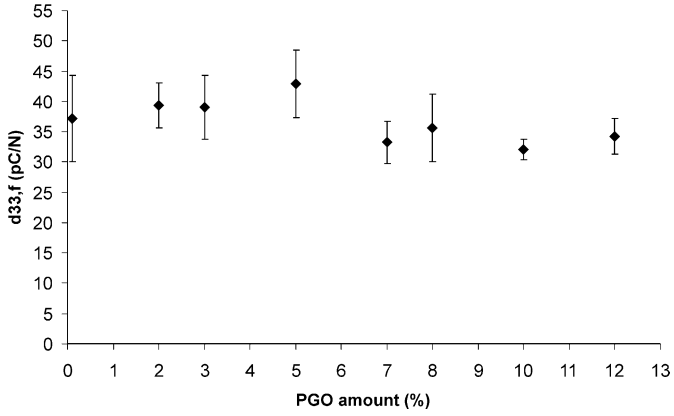

Fig. 9. Effect of PGO on the $d_{33,f}$.

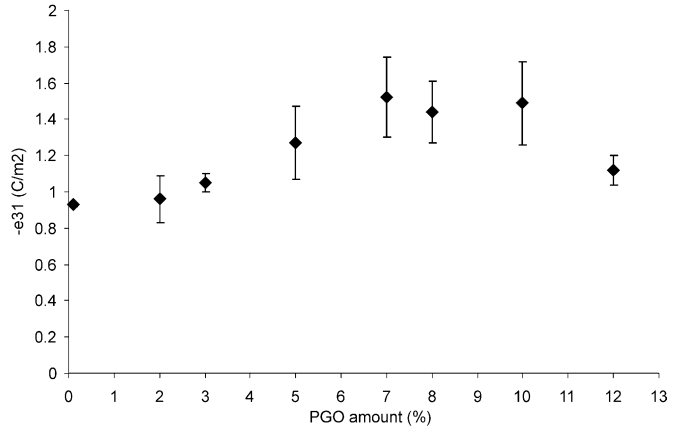

Fig. 10. Effect of PGO on $e_{31,f}$.

levels of PGO addition. It has been well established by earlier work[14] that 3-3 ceramic–air composites show reduced '3-1' piezoelectric coupling relative to dense ceramics. Hence it would be expected to see an increasing $e_{31,f}$ coefficient with increasing film density, while $d_{33,f}$ remain relatively unchanged, only decreasing at high PGO levels (as does $e_{31,f}$) due to the increasing amounts of this low permittivity, low piezoelectric coefficient phase. Interestingly the 'extrapolated' d_{33} values (representing the values for an unclamped film) follows the same trend as $e_{31,f}$. This follows from the equation for $d_{33,f}$ for the clamped film:[15]

$$d_{33,f} = d_{33,free} - \frac{2d_{31,free}{}^{*}s^{E}_{13}}{s^{E}_{11} + s^{E}_{12}} = d_{33,free} - 2e_{31,f}{}^{*}s^{E}_{13} \qquad (1)$$

where s^{E} is the compliance at constant field with the subscripts denoting the stress and strain direction.

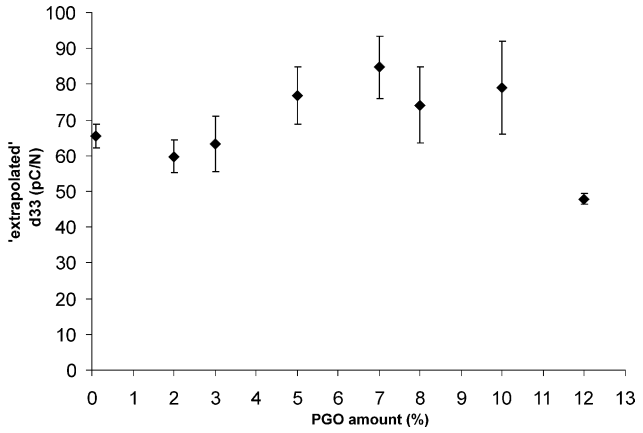

Fig. 11. Effect of PGO on 'extrapolated' d_{33}.

4. Conclusion

PGO-sinter assisted niobium-doped PZT thick films were examined as a function of the level of PGO. Incorporating 5 wt.% PGO led to the best $d_{33,f}$ piezoelectric coefficient. It has been shown that the dielectric properties were degraded when more than 8 wt.% PGO was added. Moreover it was found that the $e_{31,f}$ piezoelectric coefficient saturated for PGO addition between 7 and 10 wt.%. The deterioration of the properties at high levels of PGO is ascribed to a partial coating of the PZT grains. As the sol did not fully infiltrate the composite, the film consists of a succession of porous and dense layers. A maximum of 500, 42 pC/N and -1.5 C/m^2 were found for the relative permittivity and $d_{33,f}$ and $e_{31,f}$ piezoelectric coefficients respectively.

Addition of PGO led to an increase in the dielectric constant and $e_{31,f}$ coefficient compared with the non-assisted niobium-doped $Pb(Zr_{0.52}Ti_{0.48})O_3$ system. The densification has been improved through the use of the PGO liquid phase, but no increase in $d_{33,f}$ has been observed. The relative changes in piezoelectric coefficients with film density have been explained qualitatively in terms of a simple composite model.

Acknowledgements

The financial support of EPSRC through project GR/N05970 and the CEC through the Parmenide project is gratefully acknowledged.

References

1. Prudenziati, M., Pastes, inks and slurries. In *Thick Film Sensors*, ed. M. Prudenziati, Elsevier Science, 1994.
2. Chen, H. D. and Bernstein, J. J., Fabrication and electrical properties of lead zirconate titanate thick films. *J. Am. Ceram. Soc.*, 1996, **79**(8), 2189–2192.
3. Maas, R., Koch, M., Harris, N. R., White, N. M. and Evans, A. G. R., Thick-film printing of PZT onto silicate. *Materials Letters*, 1997, **31**, 109–112.
4. Gwirc S., Gomez H., Negreira C., Malatto L., Ultrasonic PZT gas sensor using thick film technology. In *IEEE Ultrasonics Symposium*, 1997, pp. 427–431.
5. Barrow, D. A., Petroff, T. E. and Sayer, M., Thick ceramic coating using a sol gel based ceramic-ceramic 0-3 composite. *Surface and Coating Technology*, 1995, **76-77**, 113–118.
6. Barrow, D. A., Petroff, T. E., Tandon, R. P. and Sayer, M., Characterisation of thick lead zirconate titanate films fabricated using a new sol gel based process. *J. Appl. Phys.*, 1997, **81**(2), 876–881.
7. Corker, D. L., Zhang, Q., Whatmore, R. W. and Perrin, C., PZT 'composite' ferroelectric thick films. *J. Eur. Ceram. Soc.*, 2002, **22**(3), 383–390.
8. Dorey, R. A., Stringfellow, S. B. and Whatmore, R. W., Effect of sintering aid and repeated sol infiltrations on the dielectric and piezoelectric properties of a PZT composite thick film. *J. Eur. Ceram. Soc.*, 2003, **22**, 2921–2926.
9. Watton, R., Smith, C. and Jones, G. R., Pyroelectric materials: operation and Performance in the pyroelectric camera tube. *Ferroelectrics*, 1976, **14**, 719–721.
10. Sugii, K., Iwasaki, H. and Miyazawa, S., Crystal growth and some properties of 5PbO. $3GeO_2$ single crystals. *Mater. Res. Bull*, 1971, **6**, 503–512.
11. Southin, J. E. A., Wilson, S. A., Schmitt, D. and Whatmore, R. W., $e_{31,f}$ Determination for PZT films using a conventional 'd_{33}' meter. *J. Phys. D: Appl. Phys*, 2001, **34**, 1456–1460.
12. Ferroperm—High Quality Piezoelectric Ceramic Components for the Electronics Industry (http://www.ferroperm-piezo.com/Material%20Data.html).
13. Hayashi, T., Inoue, T. and Akiyama, Y., Low temperature sintering of PZT powders coated with $Pb_5Ge_3O_{11}$ by sol-gel method. *J. Eur. Ceram. Soc.*, 1999, **19**, 999–1002.
14. Dunn, M. L. and Taya, M., Electromechanical properties of porous piezoelectric ceramics. *J. Am. Ceram. Soc.*, 1993, **76**(7), 1697–1706.
15. Steinhausen R., Hauke T., Mueller V., Beige H., Seifert S., Lobmann P., Clamping of piezoelectric thin films on metallic substrates: influence on the effective piezoelectric modulus d_{33}, applications of ferroelectrics 1998. In *ISAF 98, Proceedings of the 11th IEEE International Symposium*, pp. 93–96.